



Nonuniformities of native oxides on Si(001) surfaces formed during wet chemical cleaning

著者	伊藤 隆司
journal or publication title	Applied Physics Letters
volume	61
number	1
page range	102-104
year	1992-07-06
URL	http://hdl.handle.net/10097/34681

Nonuniformities of native oxides on Si(001) surfaces formed during wet chemical cleaning

T. Aoyama, T. Yamazaki, and T. Ito

Fujitsu Laboratories Ltd., 10-1 Morinosato-Wakamiya, Atsugi 243-01, Japan

(Received 20 January 1992; accepted for publication 20 April 1992)

We studied the uniformity of native oxide formed on Si(001) surfaces during wet chemical cleaning. Uniformity was determined by surface morphology at the initial stage of photoexcited fluorine etching. Since photoexcited fluorine etches Si 40 times faster than it etches Si oxide, it highlights Si native oxides on a Si surface making them observable by scanning tunneling microscopy or atomic force microscopy. Boiling in a $\text{HCl-H}_2\text{O}_2\text{-H}_2\text{O}$ (1:1:4) solution formed 30–70-nm islands of oxides. The regions between the islands were not oxidized. Boiling in $\text{NH}_4\text{OH-H}_2\text{O}_2\text{-H}_2\text{O}$ (1:1.4:4) also formed oxide islands 30–70 nm in diameter, but the interisland regions were slightly oxidized. Boiling in a HNO_3 solution resulted in a native oxide with pinholes at a density of $5 \times 10^9 \text{ cm}^{-2}$.

Surface cleaning is an important aspect of ultra-large-scale integration (ULSI) wafer processing. Many processes are influenced by native oxides formed during wet chemical cleaning.^{1–4} To develop new processes, a basic understanding of the formation mechanism is vital. Native Si oxides have been studied by methods including x-ray photoelectron spectroscopy (XPS), attenuated-total-reflection spectroscopy in the infrared region (ATR-IR), and thermal desorption spectroscopy (TDS).^{5–7} However, these reports remain limited to growth kinetics or chemical structure factors such as the amount of suboxides (SiO_x , $x=1-3$), silicon hydrides ($-\text{SiH}_y$, $y=1-3$), or silicon hydroxyl ($-\text{SiOH}$). Although native oxides are conventionally treated as thin, uniform films, we have actually found them to be island structures, often with many pinholes.

Figure 1 shows the oxide evaluation principle. Figure 1(a) shows island shapes and 1(b) shows pinholes. To study the shapes, we used selectively etched Si and Si oxides by photoexcited fluorine.⁸ The figures on the left-hand side are before etching and those on the right-hand side after etching. Since the photoexcited fluorine gas etches Si 40 times faster than Si oxides, the native Si oxides' shapes were clear on the Si surface and observable with scanning tunnel microscopy (STM) or atomic force microscopy (AFM). For instance, when the oxide thickness uniformity is only 0.1 nm, the difference in the Si etching depth is 4 nm.

We used *p*-type Czochralski-grown (CZ) Si (001) wafers (10 $\Omega \text{ cm}$) in our experiments. First, we cleaned the wafers by RCA processing,⁹ then dipped them in diluted HF (3:100) for 30 s. Native Si oxides were formed in three boiling stages: (1) 90 °C in $\text{HCl-H}_2\text{O}_2\text{-H}_2\text{O}$ (1:1:4) solution for 10 min, (2) 80 °C in $\text{NH}_4\text{OH-H}_2\text{O}_2\text{-H}_2\text{O}$ (1:1.4:4) solution for 10 min (NH_4OH boil), and (3) 140 °C in HNO_3 solution for 10 min. Between each step, the wafers were rinsed in de-ionized water (18 M $\Omega \text{ cm}$) for 5 min. After a final 10-min rinse the wafers were dried in a hot-nitrogen ambient. After forming native oxides using this process, atomic absorption spectrophotometry detected no metallic contaminants such as Fe, Cr, Ni, or Al on the

surface. This indicates that the levels of metallic contaminants were below $1 \times 10^{10} \text{ cm}^{-2}$.

Since details on Si etching conditions by photoexcited fluorine gas have been reported elsewhere,⁸ we will only briefly mention the conditions used here. Si was etched at atmospheric pressure. The fluorine flow rate was 2.5 ml/min (1%) and that of argon 247.5 ml/min. Fluorine was excited by ultraviolet (UV) light from low-pressure mercury lamps, whose output power at 254 nm was 24 mW/cm² on the wafer surface. Under these conditions, the steady-state etching rates were 12 nm/min for Si and 0.3

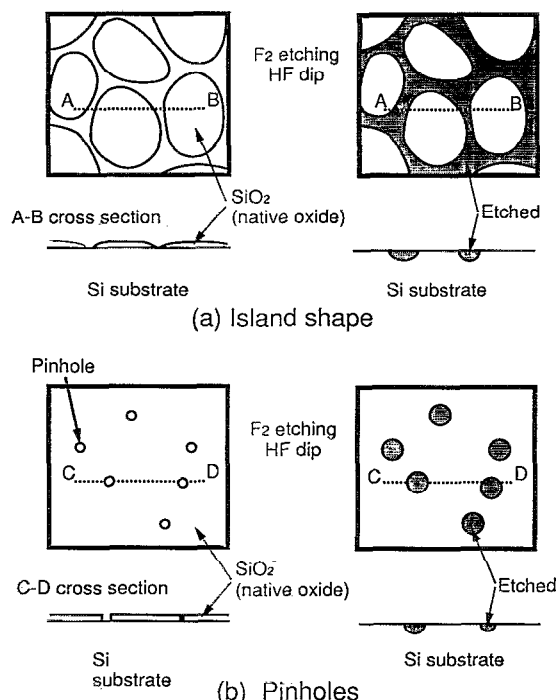


FIG. 1. Principle behind the evaluation of native oxide uniformity. Surface morphology was observed after an initial Si etching using photoexcited fluorine gas. Photoexcited fluorine etched Si 40 times faster than Si oxides, making the shape of native Si oxides clear under Si and observable using STM or AFM; (a) is the case of native oxides with an island shape and (b) is when the native oxides have pinholes.

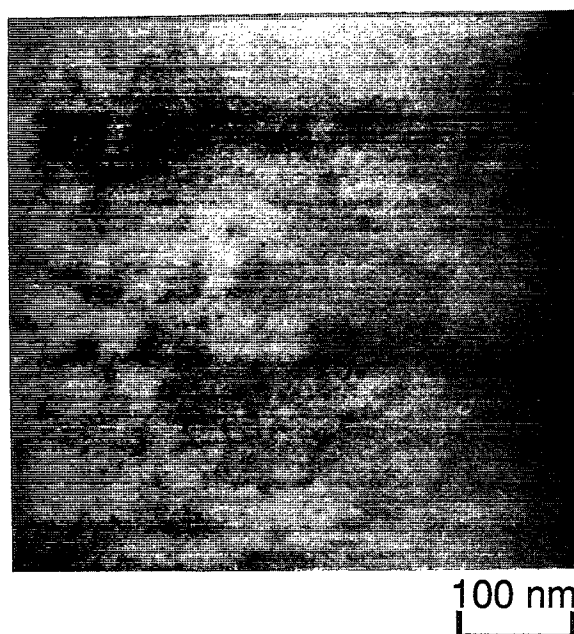


FIG. 2. STM image of the Si surface after 5 min of etching the HF-dipped wafer. No distinctive morphology was observed. The depth from white to black is 10 nm. The gray areas are in between.

nm/min for Si oxides. The Si beneath the native oxide was not etched until the native oxide was removed.

The etched surface was investigated by AFM and STM in a nitrogen ambient. Before STM observation, the etched wafers were dipped in $\text{HF-C}_2\text{H}_5\text{OH}$ (1:10) for 1 min to remove the residual native oxide and enable optimal observation of the samples.¹⁰ Before AFM observation, the samples were dipped in a diluted HF solution to remove the residual native oxide.

First, the HF-dipped wafer was etched by photoexcited fluorine gas. Almost all the dangling bonds on the surface were terminated with hydrogen.^{11–13} No distinctive morphology was observed (Fig. 2), indicating that Si etching progressed uniformly over the wafer.

Figure 3 is the Si surface after etching the HCl-boiled wafer for 5 min. The figure shows that the native oxide formed during the HCl boil had an island shape of 30–70 nm in diameter. Since we observed that Si etching started at the same time as etching for bare Si prepared by a diluted HF dip, the region between the islands was not oxidized, leaving a H-terminated Si surface.

The native oxide shape formed during NH_4OH boiling was also island shaped and had the same diameter. Regions between islands were slightly oxidized because Si etching started 3 min later than HCl boiling. Since the morphology of the NH_4OH -boiled surface was less clear than that of the HCl-boiled surface, there might be other structures which could not be observed in etching because isotropic etching by fluorine gas has left them with a high vertical but low lateral resolution.

Figure 4 shows the Si surface of a HNO_3 -boiled wafer after 12 min of etching. Many Si surface depressions were observed. Their distribution was random and their average density was $5 \times 10^9 \text{ cm}^{-2}$. This indicates that the native

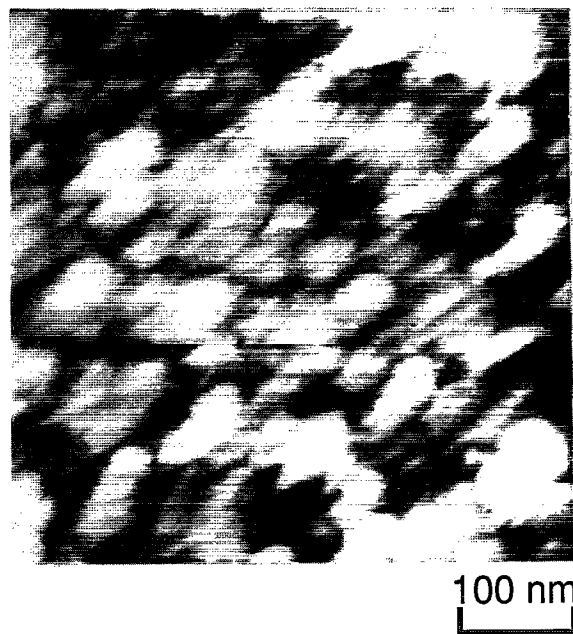


FIG. 3. STM image of the Si surface after 5 min of etching the HCl-boiled wafer. Native oxide formed during boiling in a $\text{HCl-H}_2\text{O}_2\text{-H}_2\text{O}$ (1:1:4) solution formed island shapes with 30–70 nm diameters. The depth from white to black is 10 nm.

oxide formed during HNO_3 boiling has pinholes at a density of $5 \times 10^9 \text{ cm}^{-2}$. Kobayashi *et al.* reported that voids 10^9 cm^{-2} occurred in vacuum annealing of the native oxide formed during HNO_3 boiling.¹⁴ Since their result was almost the same as ours, we presume that the voids were generated from pinholes.

In conclusion, we studied the shapes of native oxide

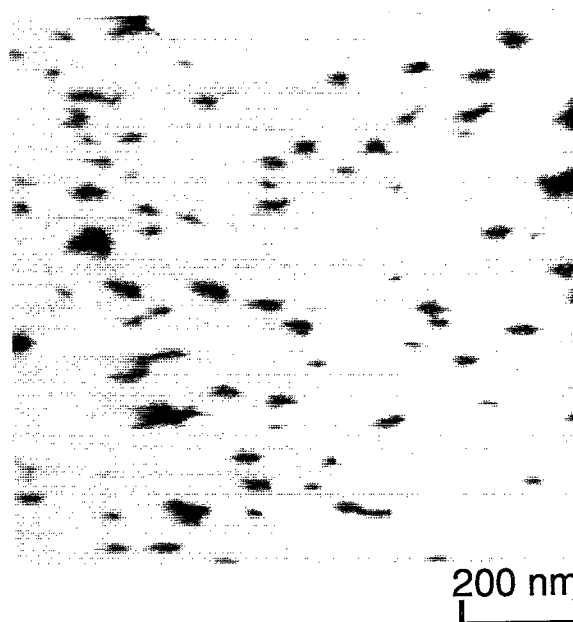


FIG. 4. AFM image of the Si surface after 12 min of etching the HNO_3 -boiled wafer. Native oxide had pinholes of average density of $5 \times 10^9 \text{ cm}^{-2}$. The depth of the depressions is 15 nm or more.

formations on Si (001) surfaces during wet chemical cleaning. The Si native oxides were not uniform, but mostly island shaped, with diameters of 30–70 nm. It was deduced that the region between the islands was not oxidized. Native oxide formed during boiling in $\text{NH}_4\text{OH-H}_2\text{O}_2\text{-H}_2\text{O}$ (1:1.4:4) had a similar shape and size, but the interisland regions were slightly oxidized. For boiling in a HNO_3 solution, the native oxide has pinholes at a density of $5 \times 10^9 \text{ cm}^{-2}$. These formations strongly influence many processes and the mechanism that binds these formations must be clarified as soon as possible.

We thank Dr. T. Sakurai for his STM observation and evaluation and thank Dr. S. Watanabe for his invaluable advice.

¹A. Ishizaka and Y. Shiraki, *J. Electrochem. Soc.* **133**, 666 (1986).

²G. Gould and E. A. Irene, *J. Electrochem. Soc.* **134**, 1031 (1987).

³E. Yablonovich, D. L. Weller, C. C. Chang, T. Gmitter, and T. B. Bright, *Phys. Rev. Lett.* **57**, 249 (1986).

⁴M. Miyawaki and T. Ohmi, *IEEE Electron Device Lett.* **EDL-11**, 448 (1990).

⁵K. Sugiyama, T. Igarashi, K. Moriki, Y. Nagasawa, T. Aoyama, R. Sugino, T. Ito, and T. Hattori, *Jpn. J. Appl. Phys.* **29**, L2401 (1990).

⁶Y. Kobayashi, and K. Sugii, *Jpn. J. Appl. Phys.* **29**, 1004 (1990).

⁷M. Morita, T. Ohmi, E. Hasegawa, M. Kawakami, and M. Ohwada, *J. Appl. Phys.* **68**, 1272 (1990).

⁸T. Aoyama, T. Yamazaki, and T. Ito, *Appl. Phys. Lett.* **59**, 2576 (1991).

⁹W. Kern and D. A. Puotinen, *RCA Rev.* **31**, 187 (1970).

¹⁰L. D. Bell, W. J. Kaiser, M. H. Hecht, and F. J. Grunthaner, *Appl. Phys. Lett.* **52**, 278 (1988).

¹¹M. Grundner and H. Jacob, *Appl. Phys. A* **39**, 73 (1986).

¹²Y. J. Chabal, G. S. Higashi, K. Raghavachari, and V. A. Burrows, *J. Vac. Sci. Technol. A* **7**, 2104 (1989).

¹³S. Watanabe, M. Shigeno, N. Nakayama, and T. Ito, *Jpn. J. Appl. Phys.* **30**, 3575 (1991).

¹⁴Y. Kobayashi and K. Sugii, *J. Vac. Sci. Technol. B* **9**, 748 (1991).